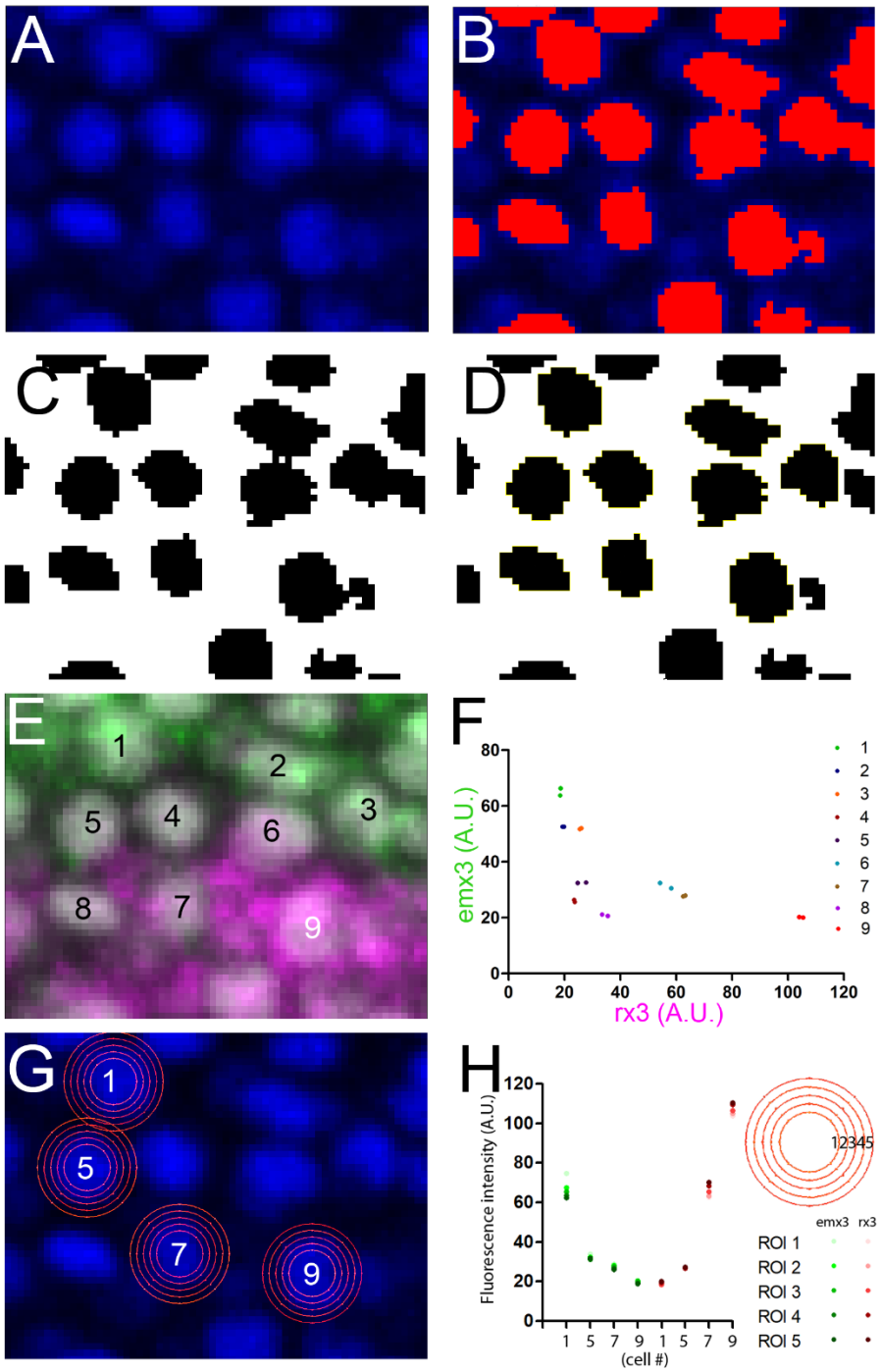

Fig. S1. Workflow for measurements of fluorescence levels in individual cells. (A) Nuclear staining with DAPI, 3µm section. (B) Thresholding of DAPI signal used for binarization. (C) Segmentation after thresholding. (D) Manual corrections after segmentation. (E) Expression of *emx3* (green) and *rx3* (magenta), individual cells are indicated with numbers. (F) Fluorescence levels in individual cells in duplicate measurements by segmentation using thresholding (A-D) and by manual segmentation. (G) Concentric ROIs of different sizes for measuring fluorescence levels. (H) Comparison of fluorescence levels measured by modifying the size of the ROI.

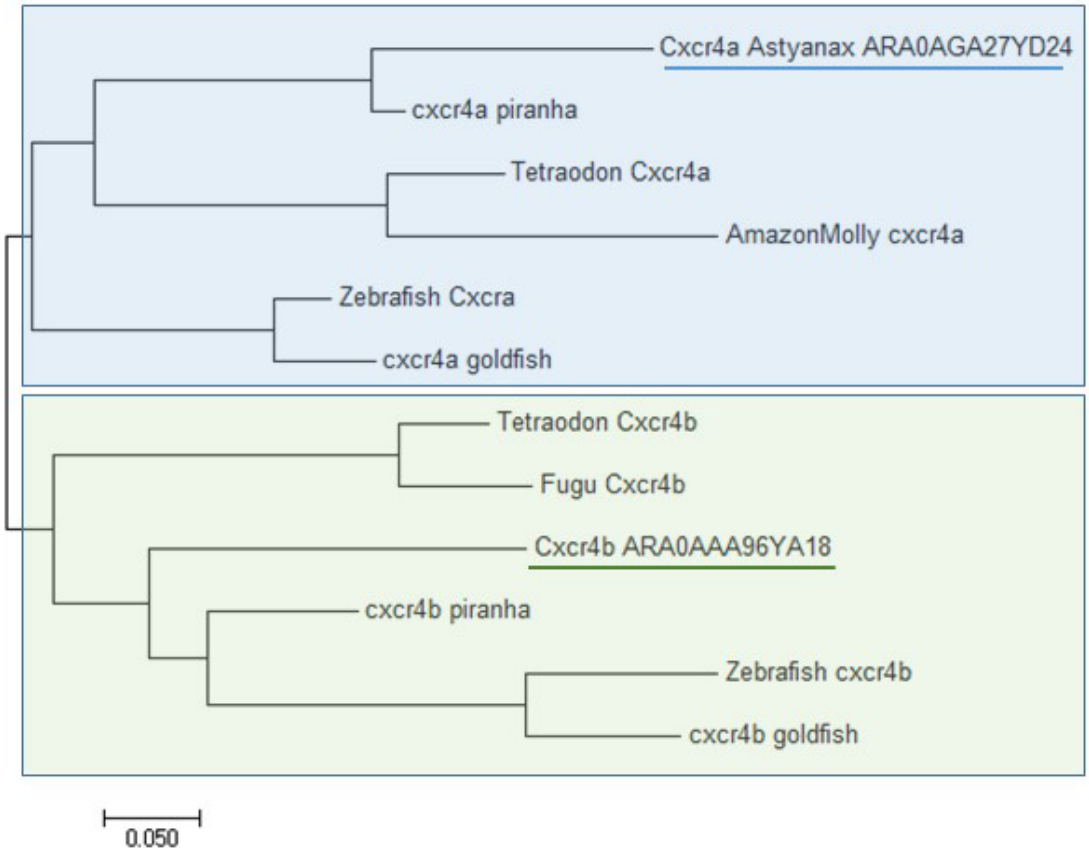

Fig. S2. Phylogenetic tree of fish Cxcr4a/b protein sequences. Maximum likelihood tree of fish Cxcr4a/b protein sequences. *Astyanax mexicanus* protein sequences (genome assembly) were deduced after sequencing of clones obtained from our cDNA library (underlined). We used *cxcr4b* in the present study.

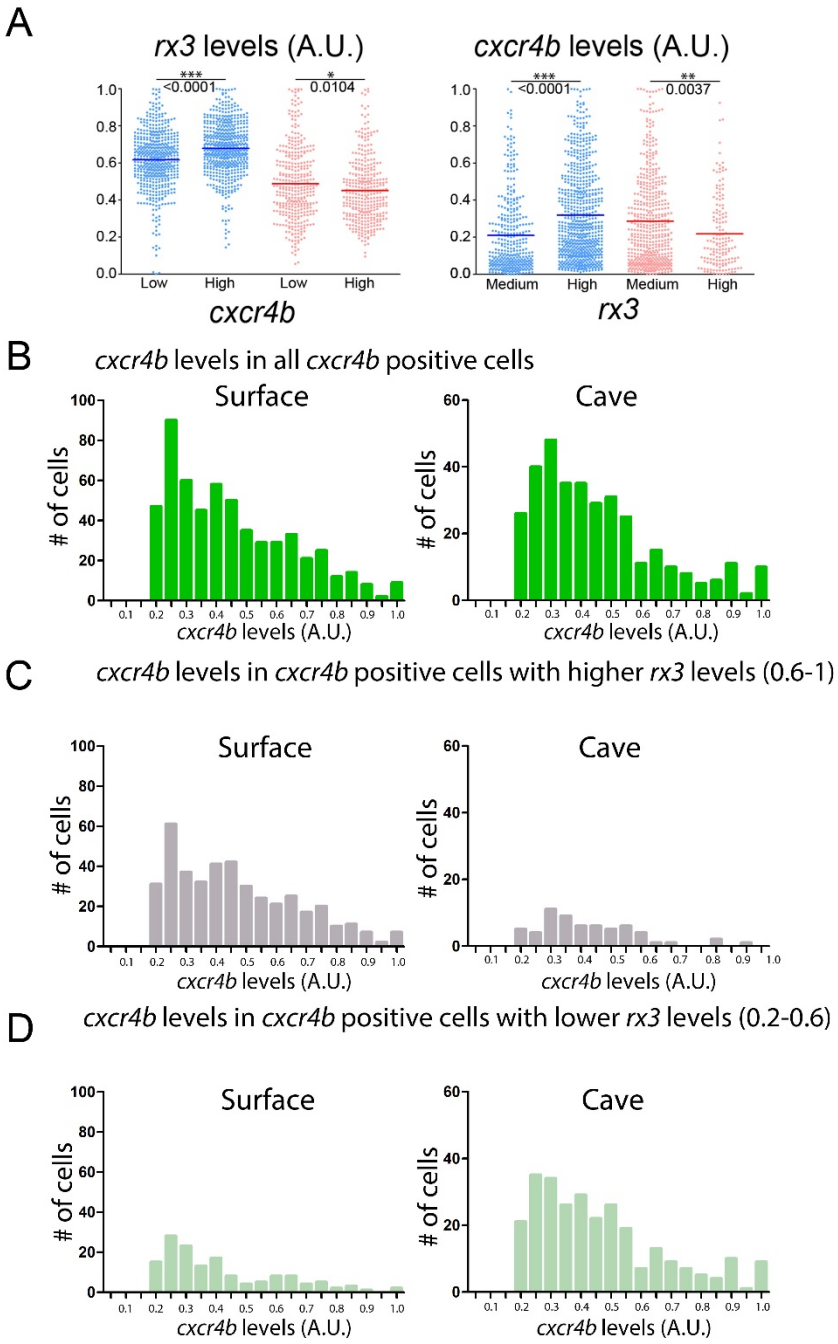

Fig. S3. Quantifications of *rx3* and *cxcr4b* levels. (A) *rx3* relative pixel intensity levels, according to low (0-0,2 AU) and higher (0.2-1 AU) *cxcr4b* levels (left) ; and *cxcr4b* relative pixel intensity levels, according to medium (0.2-0.6 AU) and high (0.6-1 AU) *rx3* levels (right), in surface fish (blue) and cavefish (red). Mean values are indicated by bars. Mann-Whitney test were performed. **(B-D)** Frequency histograms showing the distribution of cells according to different *cxcr4b* fluorescence levels (B), only for cells with high *rx3* levels (C), only for cells with lower *rx3* levels (D). All graphs correspond to ROI indicated in Figure 2I.

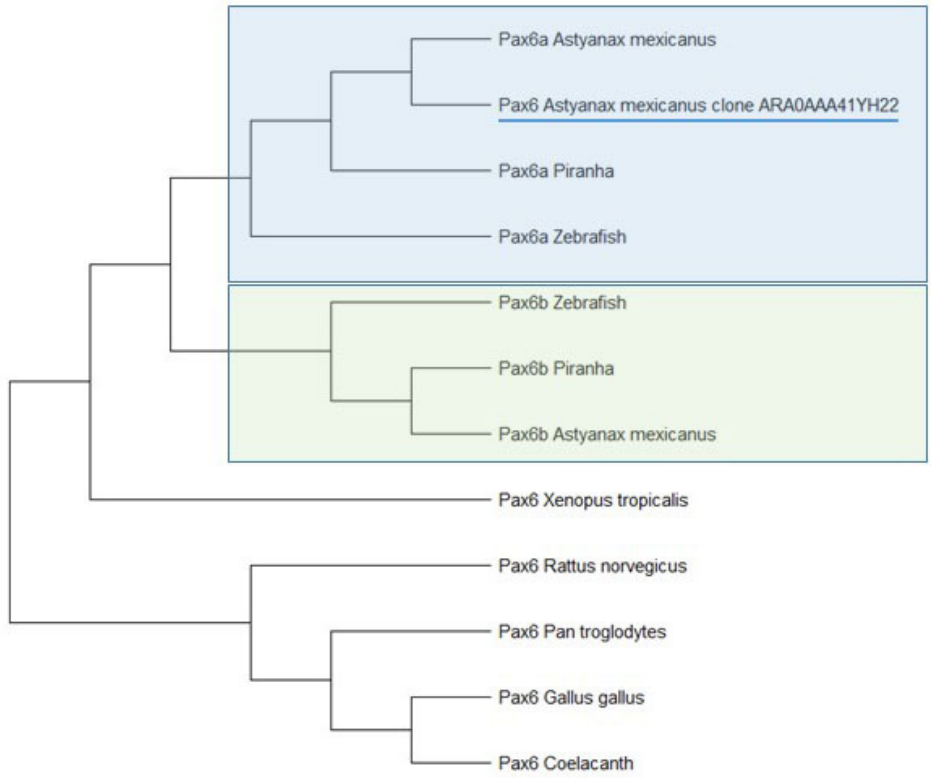

Fig. S4. Phylogenetic tree of fish Pax6a/b protein sequences. Neighbor-Joining bootstrap consensus tree on Pax6 protein alignments, performed in MEGA11. The translated protein (partial sequence, 155 amino acids) from the ARA0AAA41YH22 clone is 100% identical to the Genbank *Astyanax mexicanus pax6a* sequence.

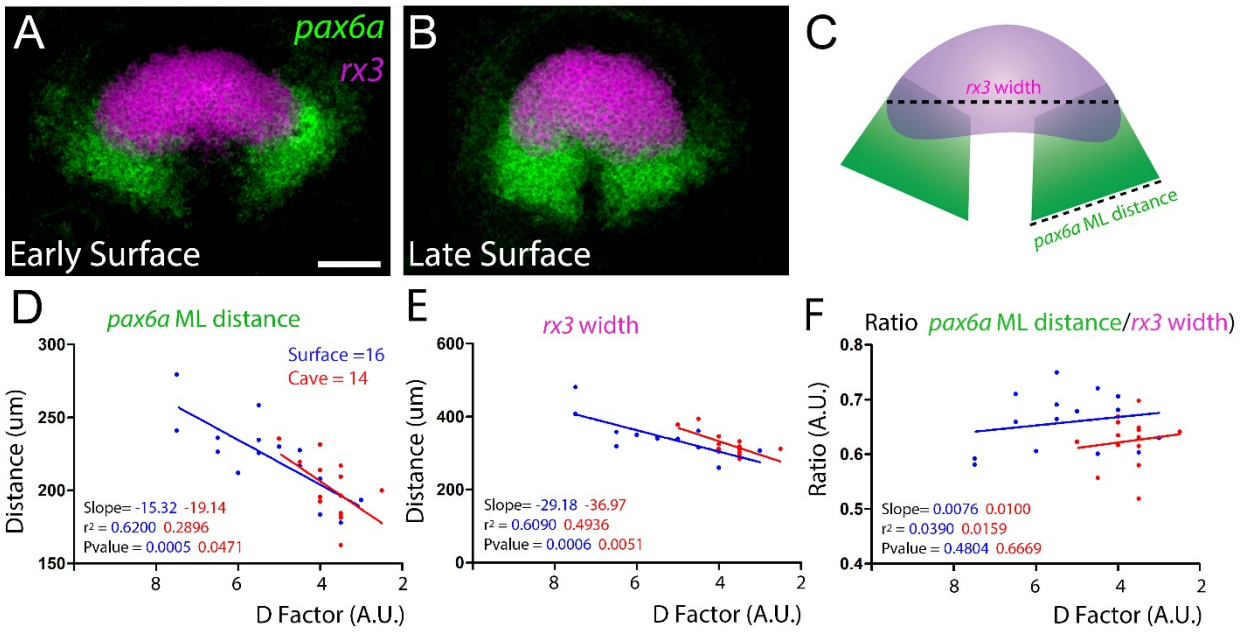

Fig. S5. Comparison of neurulation in cavefish and surface fish. (A-B) Maximum intensity projections shing the expression of *pax6a* and *rx3* in surface fish embryos at early and late neurulation states of the tailbud stage. Scheme indicating the distances measured in the *rx3* and *pax6a* expression domains. (D-F). Plots showing the pax6a ML distance (D), *rx3* width (E) and the ratio *pax6a* ML distance/*rx3* width (F) according to the different D factors. Linear regressions were calculated and the parameters obtained are indicated. Scale bar, 100µm.

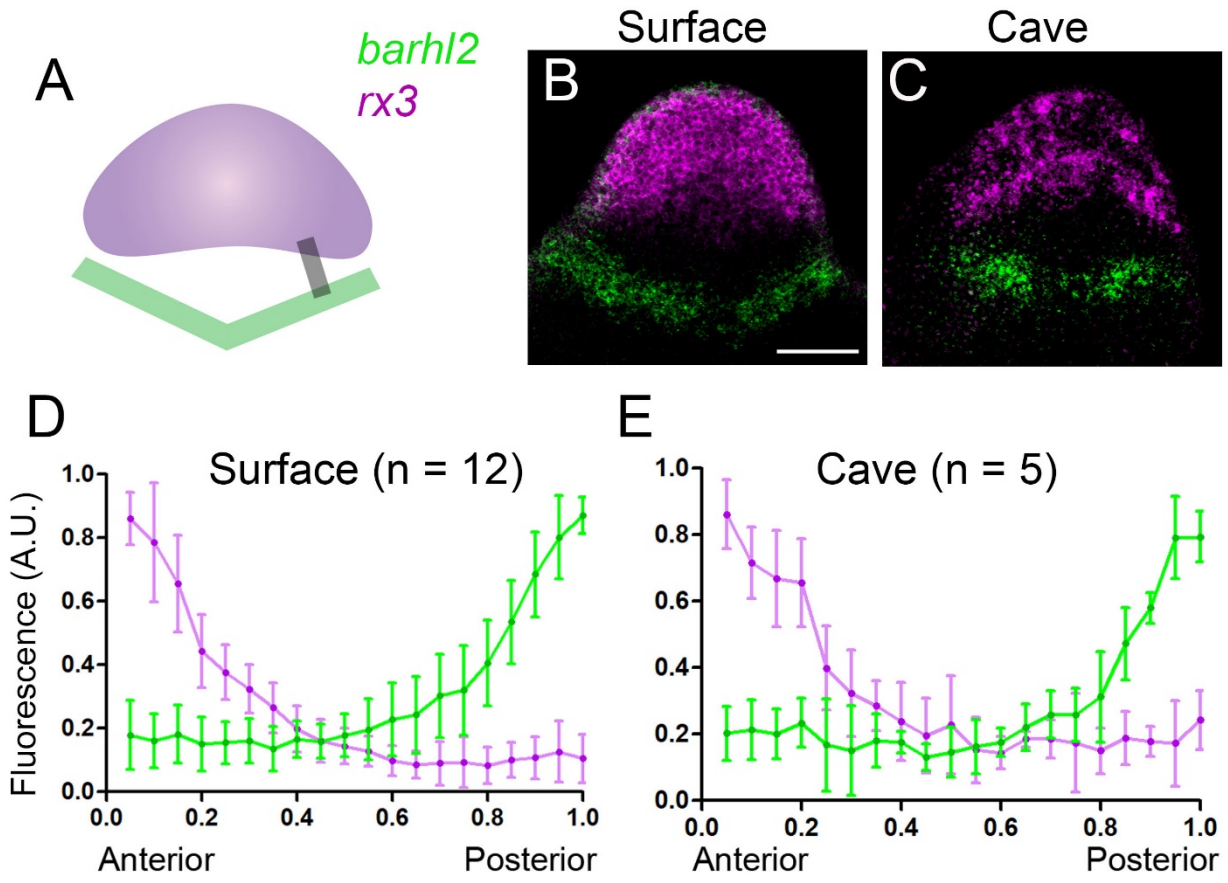

Fig. S6. Relative position of *barhl2* and *rx3* domains. (A) Scheme indicating the ROI measured covering posterior *rx3* to anterior *barhl2* domains. (B-C) Maximum intensity projections showing expression of *rx3* and *barhl2* in surface (B) and cavefish (C) embryos at 10hpf. (D-E) Fluorescence levels of *rx3* (magenta) and *barhl2* (green) according to line in (A) anterior to posterior in surface (D) and cavefish (E) embryos. Scale bar, 100µm.

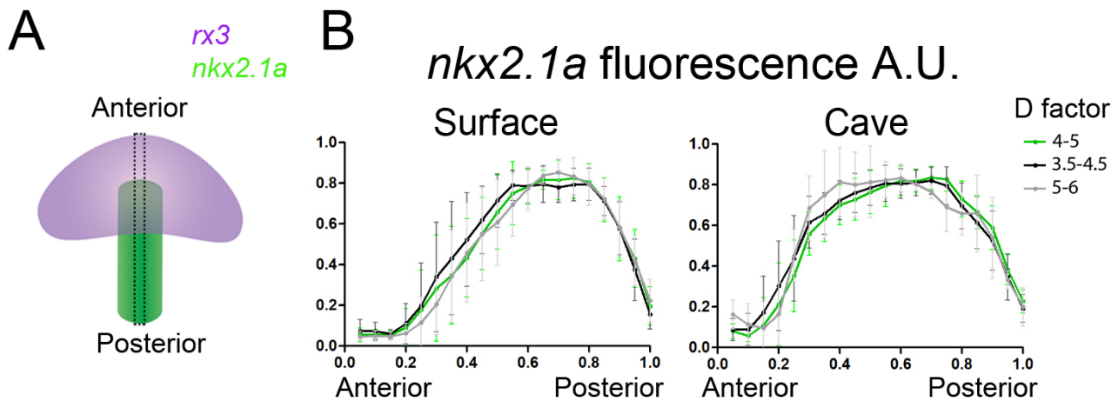

Fig. S7. Measurement of *nkx2.1a* fluorescence levels according to d factor. (A) Schematics of line A/P histogram quantification, line 50µm width from the anterior limit of *rx3* to the posterior limit of *nkx2.1a*. (B) *Nkx2.1a* fluorescence levels in surface (left) and cavefish (right) embryos according to different d factors. Two-ways ANOVA tests were performed.

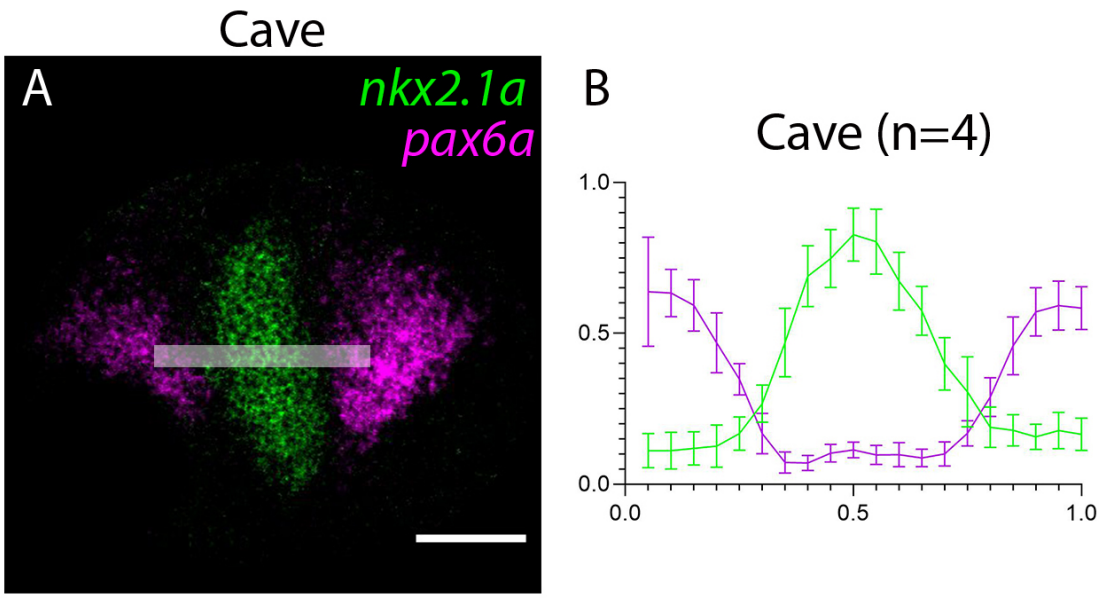

Fig. S8. Relative position of *pax6a* and *nkx2.1a* domains in the cave morph. (A) Maximum intensity projections of an intermediate substack (3 μm). (B) Plot profiles for *pax6a* and *nkx2.1a* (rectangle in A, 10 μm wide). As evidenced, a gap separates both domains in this morph, where *nkx2.1a* domain is expanded compared to surface fish. Scale bar 100 μm.

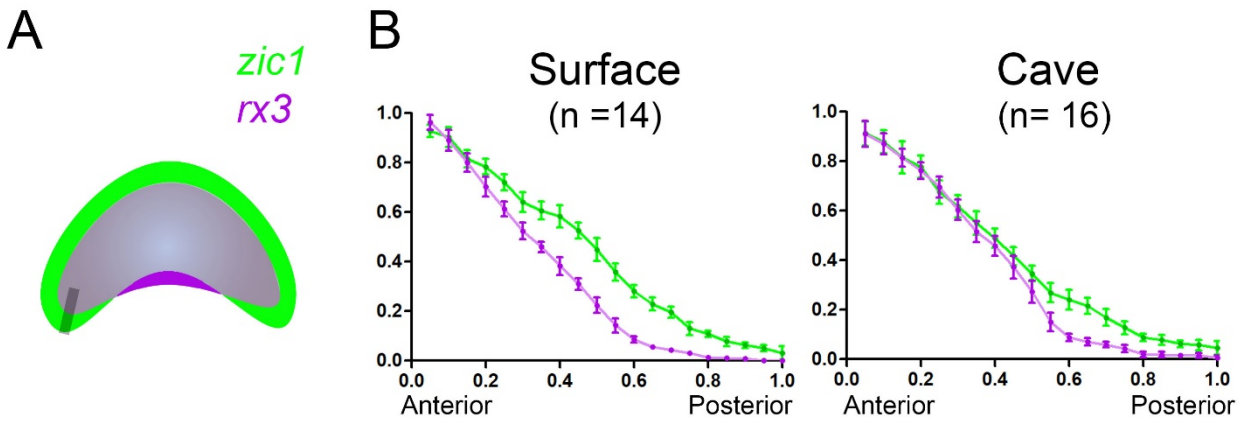

Fig. S9. Measurement of *zic1* and *rx3* fluorescence levels at the posterior limit of the eyefield. (A) Schematics of line A/P histogram quantification, line of 80µm width at the posterior limit of *zic1*. (B) *zic1* (green) and *rx3* (magenta) fluorescence levels in surface (left) and cavefish (right) embryos in the posterior limit of the eyefield (line in A).

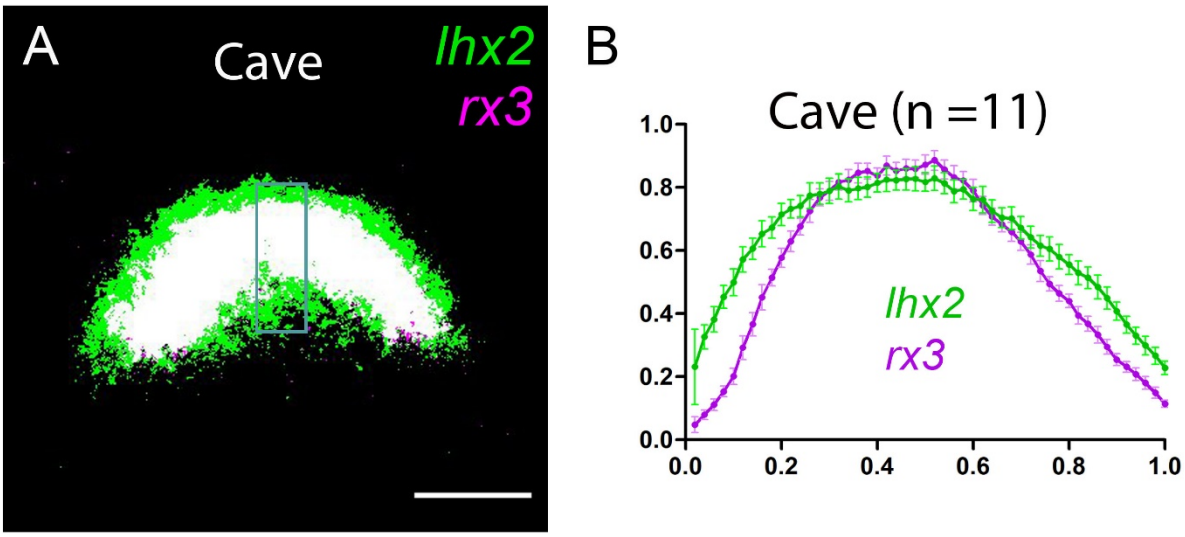

Fig. S10. Measurement of *lhx2* and *rx3* fluorescence levels at the ANP midline in cavefish. (A) Binary image of a full stack maximum intensity projection showing anterior position of lhx2 expression domain compared to *rx3* in cavefish. (B) Averaged plot profile according to ROI (A, rectangle) for the indicated number of cavefish samples.

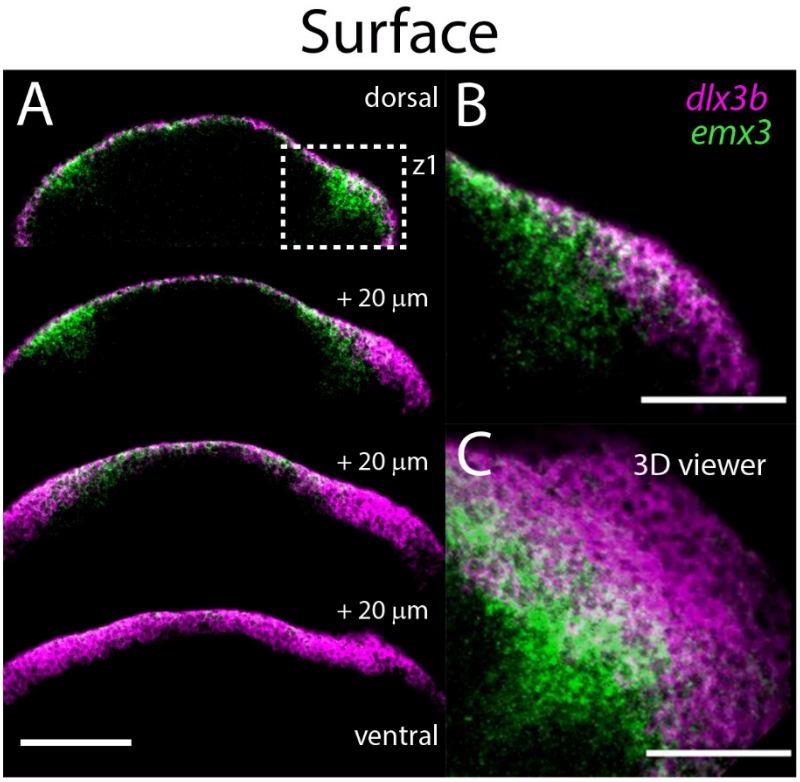

Fig. S11. Images of double fluorescent ISH showing *dlx3b* and *emx3* relative lateral posterior positions in the ANP. (A) Montage of 4 different maximum intensity projections (3 µm) in the DV axis. (B-C) Dorsal views of 3D renditions obtained by 3D stack projection (B) and 3D stack viewer (C) corresponding to square in A. Scale bar, 100 µm.

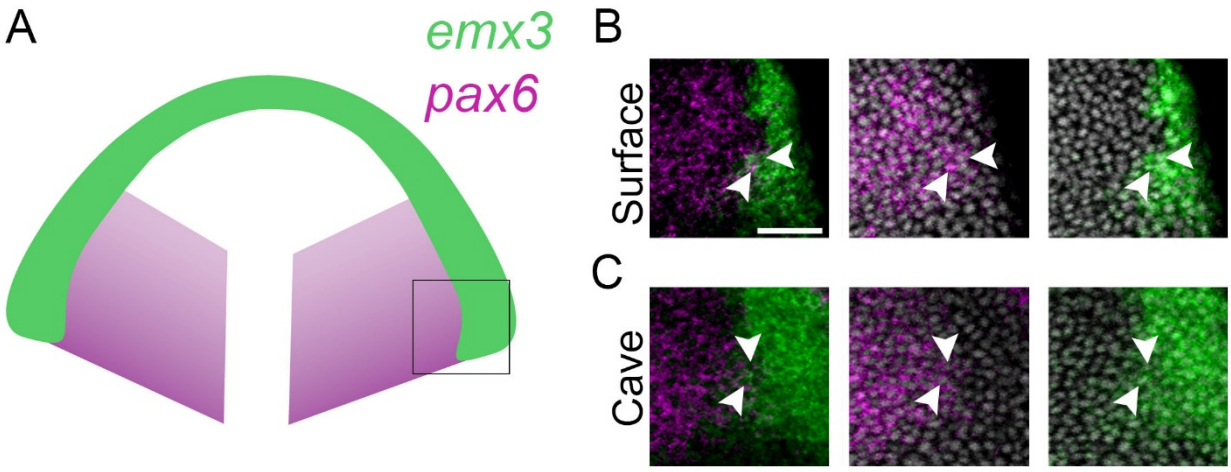

Fig. S12. Existence of a small *pax6a* and *emx3* lateral posterior domain in the ANP. (A) Schematics of the *emx3* and *pax6* expression domains. Black square indicates the region that is zoomed in B-C. (B-C) expression of *emx3* and *pax6* in the posterior ANP domain in surface fish (B) and cavefish (C). Arrowhead point to cells expressing both markers. Staining with DAPI was used to identify individual nuclei (greys). Scale bar, 50 µm.

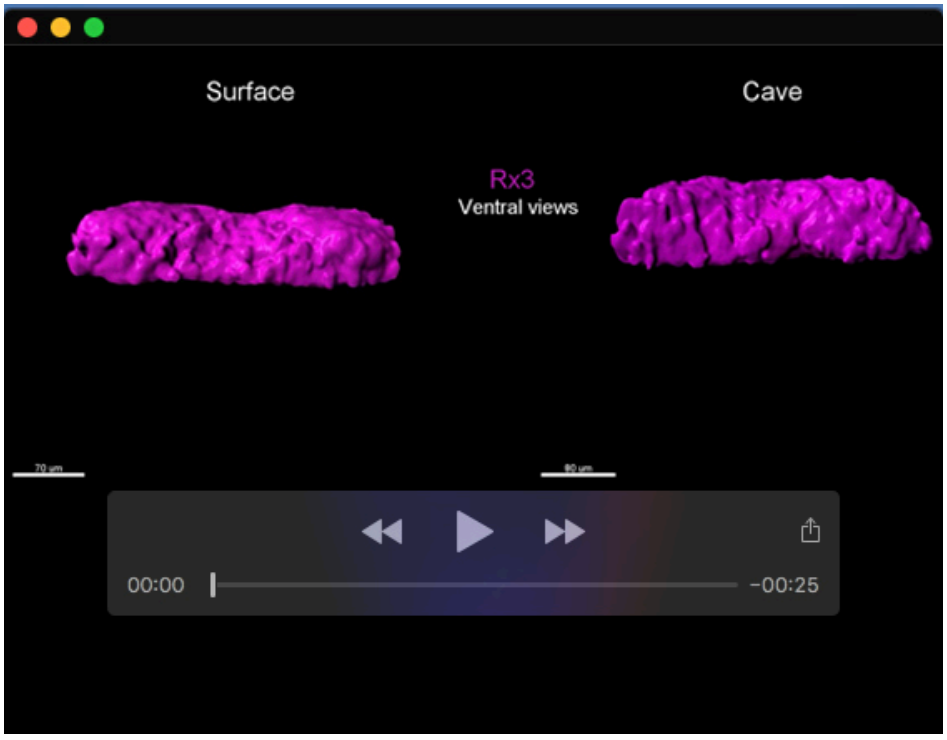

Movie 1. Comparison of *rx3* domain 3D shape in surface fish and cavefish.

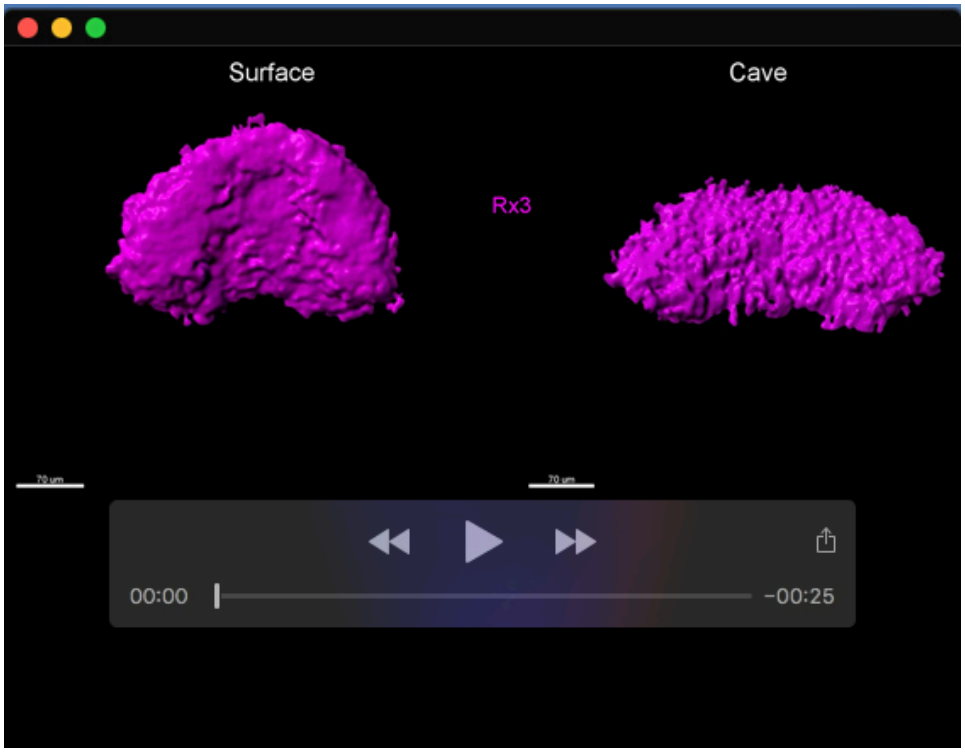

Movie 2. Highlighting *cxcr4b* subdomain in surface fish and cavefish.

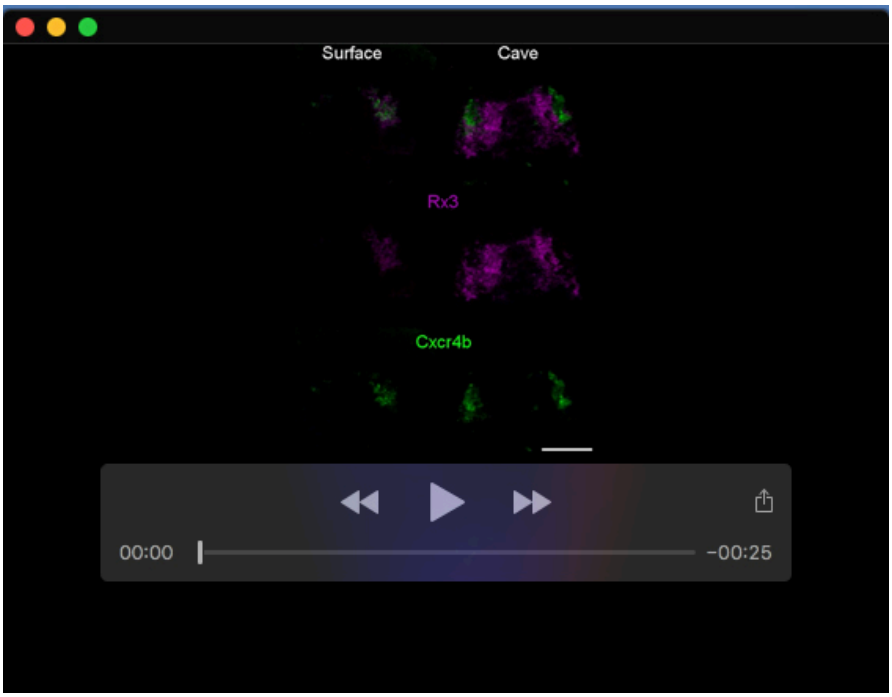

Movie 3. Highlighting *cxcr4b* and *rx3* complementary expression in cavefish ANP.

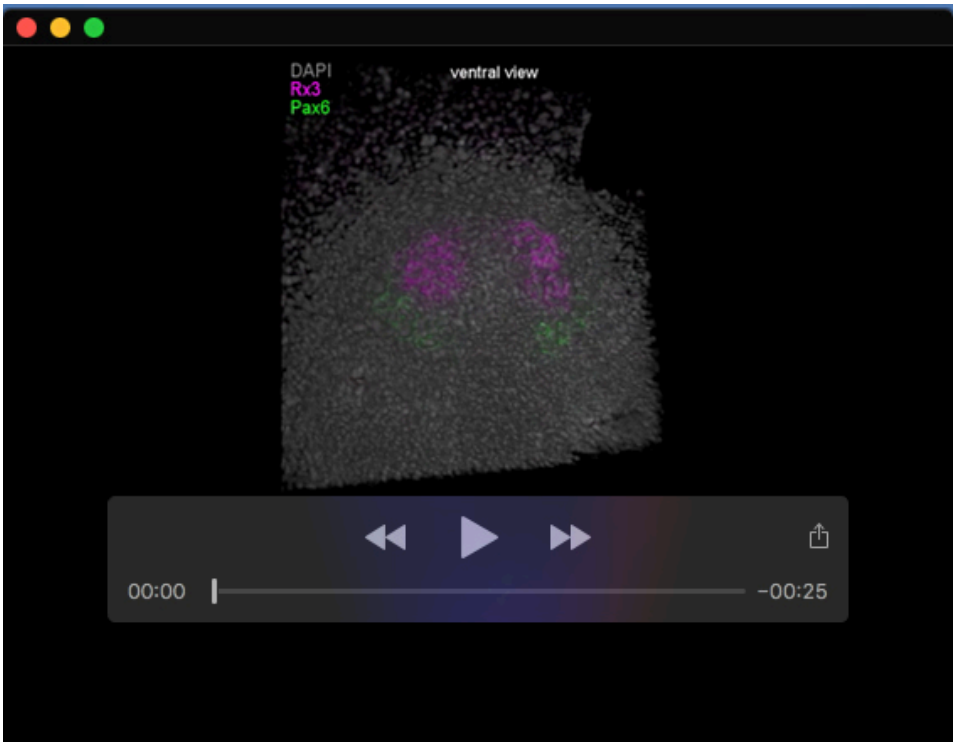

Movie 4. Anteroposterior eyefield regionalization in 3D.

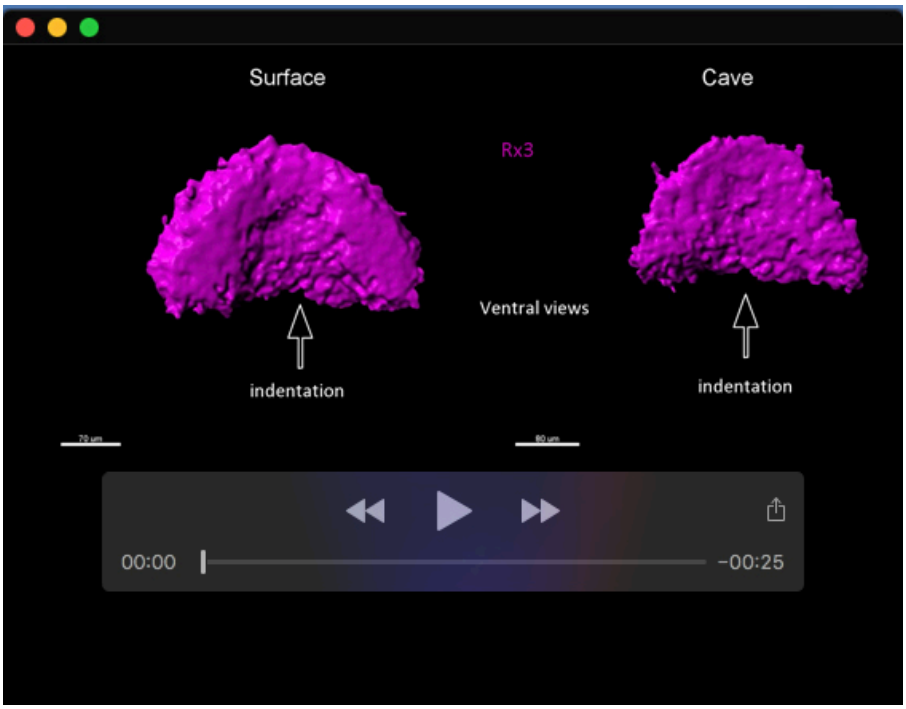

Movie 5. Relative position of the prospective hypothalamus and eyefield in 3D and domain interface size and shape.

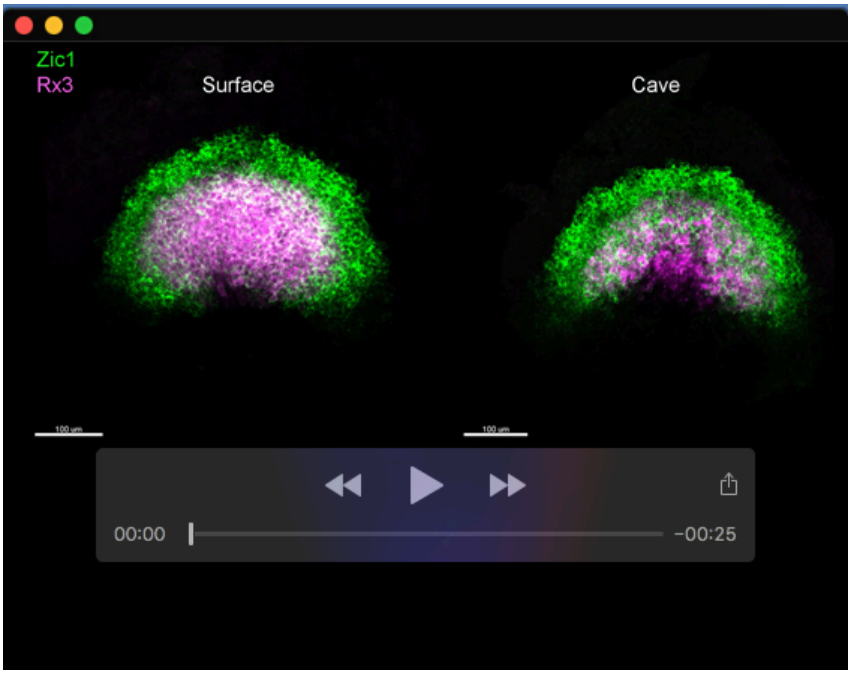

Movie 6. Major subdivisions in the anterior eyefield revealed by *zic1* and *rx3*.

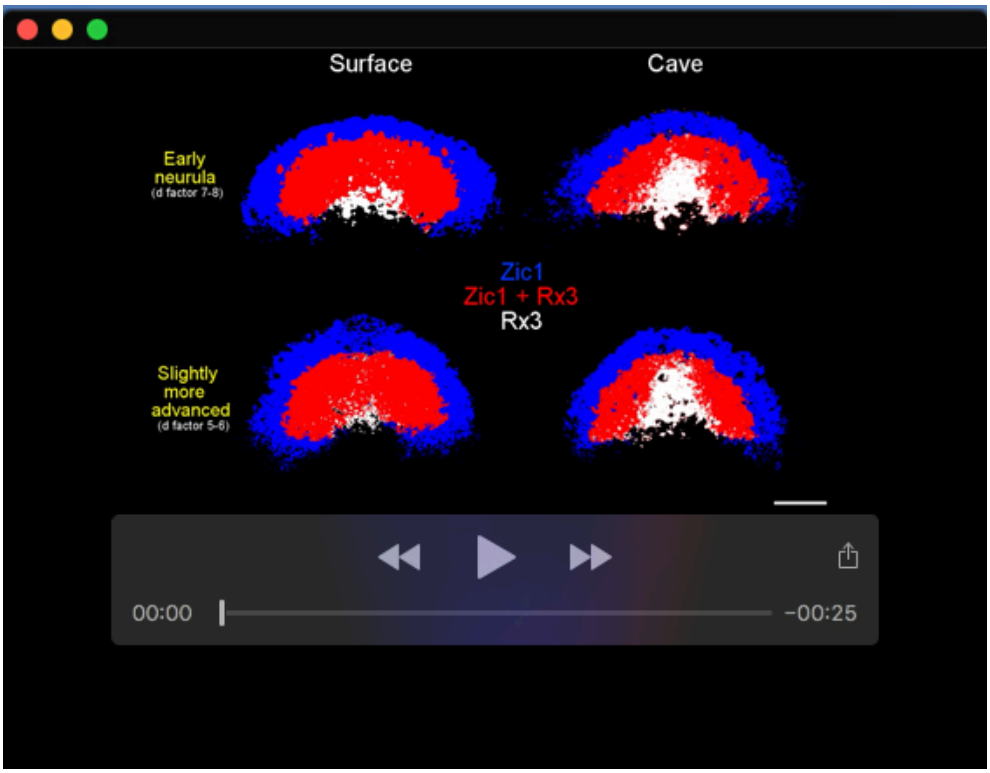

Movie 7. Enlargement of the only *rx3*-expressing ventral midline eyefield subdivision in cavefish.

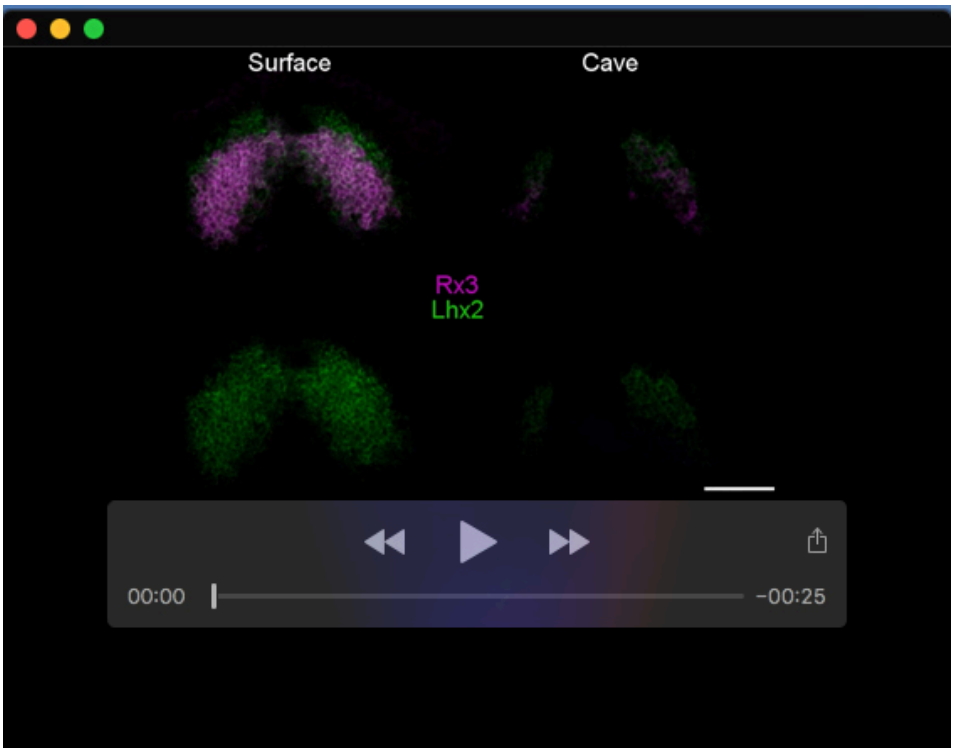

Movie 8. Highlighting slight anterior position of *lhx2* expression in surface fish and cavefish ANP.

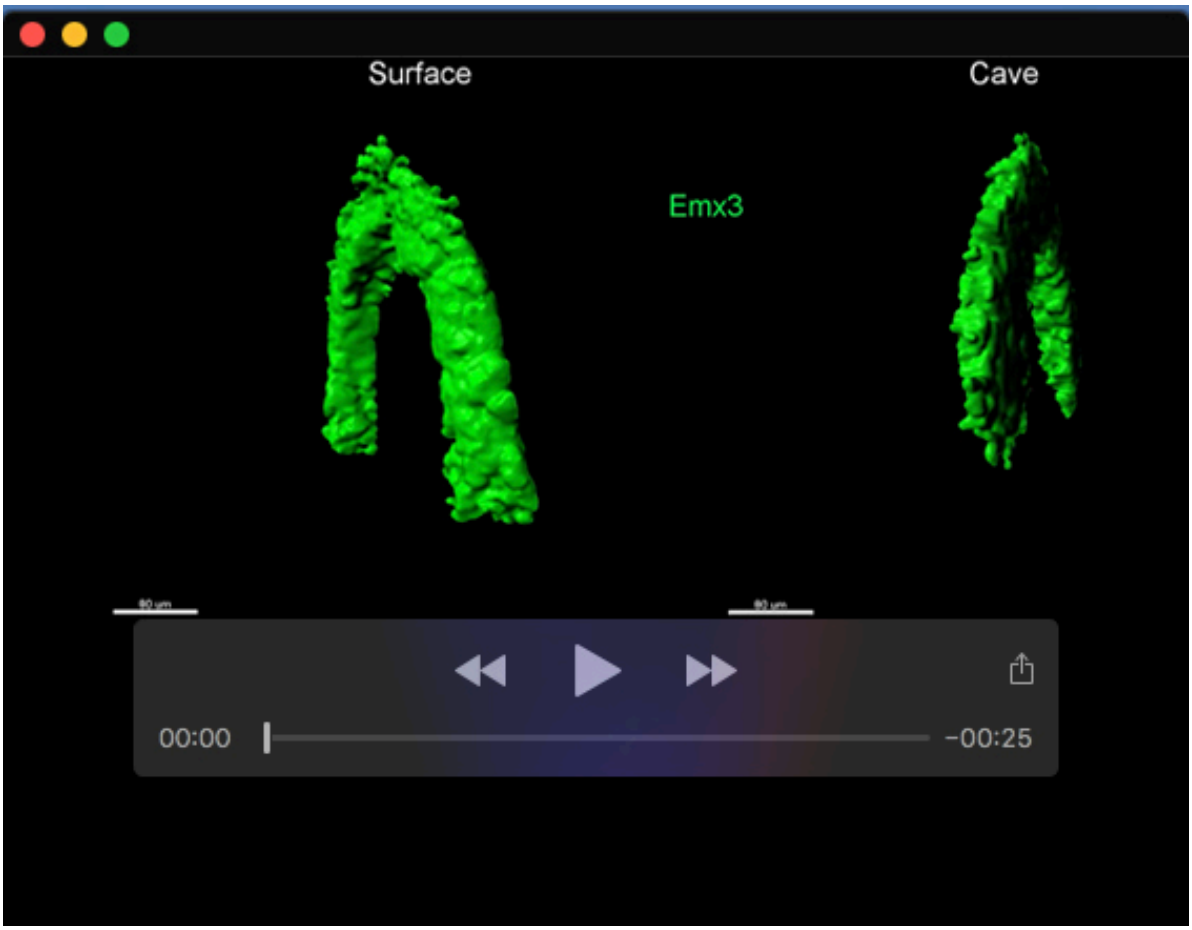

Movie 9. 3D comparison of the eyefield and prospective telencephalon interface in surface fish and cavefish.